1   **Inter-comparison of online and offline methods for measuring ambient heavy and trace elements**

2   **and water-soluble inorganic ions (NO$_3^-$, SO$_4^{2-}$, NH$_4^+$ and Cl$^-$) in PM$_{2.5}$ over a heavily polluted**

3   **megacity, Delhi**

4   Himadri Sekhar Bhowmik[1], Ashutosh Shukla[1], Vipul Lalchandani[1], Jay Dave[2], Neeraj Rastogi[2], Mayank

5   Kumar[3], Vikram Singh[4], and Sachchida Nand Tripathi[1*]

6   [1] Department of Civil Engineering, Indian Institute of Technology Kanpur, Kanpur, India

7   [1*] Department of Civil Engineering and Centre for Environmental Science and Engineering, Indian

8   Institute of Technology Kanpur, Kanpur, India

9   [2] Geosciences Division, Physical Research Laboratory, Ahmedabad, India

10   [3]Department of Mechanical Engineering, Indian Institute of Technology Delhi, New Delhi, India

11   [4]Department of Chemical Engineering, Indian Institute of Technology Delhi, New Delhi, India

12   *Correspondence to:* S. N. Tripathi (snt@iitk.ac.in)

13   Keywords: Aerosol mass spectrometer (AMS), Xact 625i ambient metal mass monitor, Ion

14   Chromatography (IC), ICP-MS, elemental composition.

15   **Abstract**

16   Characterizing the chemical composition of ambient particulate matter (PM) provides valuable

17   information on the concentration of secondary species, toxic metals and assists in the validation of

18   abatement techniques. The chemical components of PM can be measured by sampling on filters and

19   analysing them in the laboratory or using real-time measurements of the species. It is important for the

20   accuracy of the PM monitoring networks that measurements from the offline and online methods are

21   comparable and biases are known. The concentrations of water-soluble inorganic ions (NO$_3^-$, SO$_4^{2-}$, NH$_4^+$

22   and Cl$^-$) in PM$_{2.5}$ measured from the 24 hrs filter samples using ion chromatography (IC) were compared

23   with the online measurements of inorganics from aerosol mass spectrometer (AMS) with a frequency of 2

24   mins. Also, the concentrations of heavy and trace elements determined from the 24 hrs filter samples

25   using inductively coupled plasma mass spectroscopy (ICP-MS) were compared with the online

26   measurements of half-hourly heavy and trace metal's concentrations from Xact 625i ambient metal mass

27   monitor. The comparison was performed over two seasons (summer and winter) and at two sites (Indian

28   Institute of Technology, Delhi and Indian Institute of Tropical Meteorology, Delhi) which are located in

29   Delhi, NCR, India, one of the heavily polluted urban areas in the world. Collocated deployments of the
30   instruments helped to quantify the differences between online and offline measurements and evaluate the
31   possible reasons for positive and negative biases. The slopes for SO_4^{2-} and NH_4^+ were closer to 1:1 line
32   during winter and decreased during summer at both sites. The higher concentrations on the filters were
33   due to the formation of particulate $(NH_4)_2SO_4$. Filter-based NO_3^- measurements were lower than online
34   NO_3^- during summer at IITD and winter at IITMD due to the volatile nature of NO_3^- from the filter
35   substrate. Offline measured Cl^- was consistently higher than AMS derived Cl^- during summer and winter
36   at both sites. Based on their comparability characteristics, elements were grouped under 3 categories. The
37   online element data were highly correlated ($R^2 > 0.8$) with the offline measurements for Al, K, Ca, Ti, Zn,
38   Mn, Fe, Ba, and Pb during summer at IITD and winter at both the sites. The higher correlation
39   coefficient demonstrated the precision of the measurements of these elements by both Xact 625i
40   and ICP-MS. Some of these elements showed higher Xact 625i elemental concentrations than ICP-MS
41   measurements by an average of 10-40% depending on the season and site. The reasons for the differences
42   in the concentration of the elements could be the distance between two inlets for the two methods, line
43   interference between two elements in Xact measurements, sampling strategy, variable concentrations of
44   elements in blank filters and digestion protocol for ICP measurements.

1. Introduction

46   The adverse effect of ambient particulate matter (PM) on human health and the role of PM in visibility
47   degradation, altering earth's radiation balance, and climate change has received global attention in the last
48   two decades (Pope et al., 2009; Hong et al., 2019; Wang et al., 2019). To gain better insight into their
49   properties, the chemical characterization of particulate matter and its source attribution is crucial. The
50   National Capital Region (NCR), which includes India's capital (New Delhi) along with some districts
51   (Gurugram, Faridabad, and Noida) of the adjoined states of Haryana, Rajasthan, and Uttar Pradesh, is one
52   of the most polluted urban areas in northern India with a population over 47 million (Bhowmik et al.,
53   2021). According to World Economic Forum, New Delhi was listed as the most polluted city globally,
54   with an annual average $PM_{2.5}$ concentration of ~140 μg m^{-3} (World Health Organisation, 2018). NCR has
55   been a specific area for researchers for the past couple of years due to its unprecedented $PM_{2.5}$ levels.
56   Various large and small scale industries, power plants, construction activities, and rapid increase in the
57   vehicle numbers (11 million in 2018) (Rai et al., 2020) are among the several causes that massively
58   reduces the air quality index (AQI) (Rai et al., 2020; Sharma & Kulshrestha, 2014). Further, the crop
59   residue burning during the month of Oct-Nov in the adjoining states of Haryana and Punjab on a larger
60   scale worsens the air quality.

For decades, the mass concentrations of major water soluble inorganic ions (WSIS) and heavy and trace metals in PM have been carried out by sampling them on filters and subsequently analysing them in laboratory. Water-soluble inorganic ions (WSIS) and heavy and trace elements from these filter samples are analyzed using ion chromatography (IC) (Bhowmik et al., 2021; Rengarajan et al., 2007; Rastogi & Sarin, 2005) and inductively coupled plasma-mass spectroscopy (ICP-MS) or inductively coupled plasma-optical emission spectroscopy (ICP-OES) (Patel et al., 2021) respectively. Usually, these filters are collected over 24 hrs interval. Traditional receptor models usually use these offline measured data of very low temporal resolution, making it challenging to characterize the short pollution episodes and dynamics of pollution sources. Further, un-denuded filter sampling can have both negative and positive artifacts due to volatile species (Lipfert, 1994; Pathak & Chan, 2005). The absorption of acidic and alkaline gases on the filter substrates, if not removed prior to sampling, can give positive artifacts and result in overestimating species concentration. Likewise, the evaporation of semi-volatile compounds (ammonium nitrate) from filter substrates can give negative biases and result in underestimating aerosol concentration and its species (Pathak & Chan, 2005; X. Zhang & Mcmurryt, 1992). The degree of artifacts can be affected by several factors, including temperature, relative humidity, type of filter substrate, the aerosol loading on the filter substrate, etc. Transient events can also lead to mismatch. To overcome the limitations of low temporal resolution and avoid the artifacts associated with offline filter sampling, methods have been developed for measuring aerosol chemical composition at a higher time resolution in the order of hours or minutes.

Aerosol Mass Spectrometer (AMS) (Canagratna et al., 2007; Jayne et al., 2000; Jimenez et al., 2003) is one kind of such instrument, which provides size-resolved chemical composition of non-refractory submicron aerosols, e.g., organics, sulphate, nitrate, ammonium, and chloride at the order of hours or even minutes. For other important components, such as calcium (main constituents of soil dust and construction activities) and potassium (tracer of biomass burning), which AMS cannot measure, Xact ambient metal mass monitor can be used. It is capable of measuring 45 elements, e.g., Al, Si, P, S, Cl, K, Ca, Ti, V, Cr, Mn, Fe, Co, Ni, Cu, Zn, Ga, Ge, As, Se, Br, Rb, Sr, Y, Zr, Nb, Mo, Pd, Ag, Cd, In, Sn, Sb, Te, I, Cs, Ba, La, Ce, Pt, Au, Hg, Tl, Pb and Bi with a frequency of every 30 mins to 4 hours. However, the high time-resolution instruments measure lower range of species concentrations with higher limit of detection (LOD) than the offline based methods (Tremper et al., 2018). Both offline and online methods have their own strength and weaknesses. Uncertainties in offline filter analysis methods have been extensively studied (Pathak & Chan, 2005; Viana et al., 2006), but the novel online methods pose new problems (Wu & Wang, 2007). For example, when the ambient concentrations are very low, online measurements are often close to the MDL values due to the short integration times (Malaguti et al., 2015).

94 Previous studies in Delhi-NCR have used low time resolution filter-based methods for chemical
95 characterization of submicron aerosols (Bhowmik et al., 2020; Nagar et al., 2017; Pant et al., 2015; S. K.
96 Sharma et al., 2016; Singhai et al., 2017). On the other hand, there are only a few studies in Delhi-NCR
97 that used high time resolution methods (HR-ToF-AMS, Q-ACSM, Xact) for characterization and source
98 apportionment of coarse and fine particulate matters (Gani et al., 2019; Lalchandani et al., 2021; Rai et
99 al., 2020, 2021; Singh et al., 2021; Tobler et al., 2020). Online and offline measurements both have their
100 advantages and limitations. For both these measurements, the quality of the data highly depends on the
101 calibration of the instruments. For Xact, the multi-element mix standard might not represent ambient
102 elemental mix if the ambient particulate matters are too low or too high in concentration, affecting the
103 collection properties of the filter (Indresand et al., 2013). For filter-based water-soluble inorganic ion and
104 metal analysis, confidence in the data depends on the calibration as well as the volatility, solubility, and
105 digestion protocol used for the extraction of water-soluble inorganic ions and elements, respectively.
106 Thus, it is vital for monitoring networks that both the offline and online measurement methods give
107 comparable results. Few published studies have compared inorganics and elements from filter-based
108 measurements and semi-continuous methods (e.g., Furger et al., 2017; Nie et al., 2010). The inter-
109 comparison in these studies is unjustified for highly polluted areas, as the specie values observed in these
110 studies are much below MDL due to very low ambient concentration of secondary species and elements.
111 It will be interesting to study the inter-comparison in highly polluted areas. To the best of our knowledge,
112 there are neither any published seasonal and temporal comparisons of inorganics from high time
113 resolution AMS measurements and filter-based measurements from ion chromatography nor any
114 comparisons of heavy and trace metals from high time resolution Xact 625 ambient metal mass monitor
115 and offline measurements from ICP-MS in the heavily polluted Delhi NCR region.

116 This study demonstrates a comparison between online and offline measurements of WSIS and heavy and
117 trace metals at two sites in Delhi NCR during summer (June-July 2019), characterized by moderate levels
118 of local pollution and winter (October-December 2019), affected by high levels of pollution from local
119 sources and regional transport of crop residue burning emissions from adjoining state of Haryana and
120 Punjab.

2. Methodology

2.1. Sampling sites

123 Delhi-NCR, a highly polluted urban area with an annual average $PM_{2.5}$ concentration of 140 μg m^{-3} and a
124 population of over 47 million, is surrounded by the Thar desert on its west and Indo-Gangetic Plain on its

125 east to south-east. The temperature is about ~35°C-48°C during summer (April-June), and winter
126 (December-February) is relatively cooler, with temperature ranges from ~2°C-15°C (Bhowmik et al.,
127 2020; Vipul Lalchandani et al., 2021; Tobler et al., 2020). The wind is mostly north-westerly during both
128 summer and winter.

129
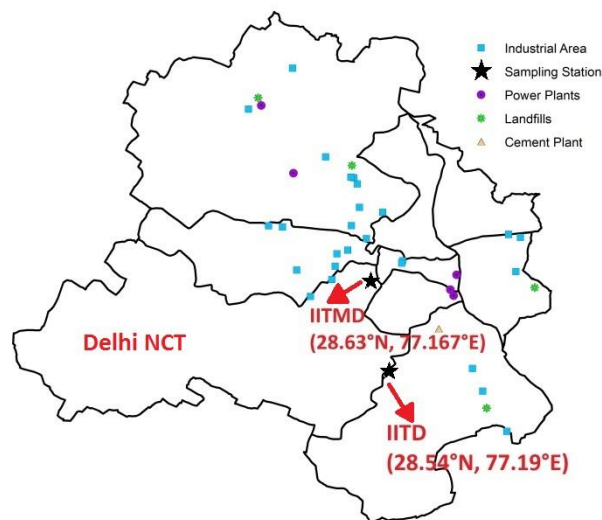
130   Fig.1. Sampling sites with various emission sources like power plants, industries, landfills, etc.

131 **2.1.1. Delhi NCR site 1: IITD**

132 High volume PM$_{2.5}$ samples were collected on the rooftop of the Centre for Atmospheric Science (CAS)
133 building at the Indian Institute of Technology, Delhi (IITD) (28.54°N, 77.19°E; ~218 m amsl) about ~15
134 m above the ground level. Further, one HR-ToF-AMS and Xact ambient metal mass monitor were
135 deployed inside a temperature-controlled laboratory on the 3rd floor of the same building about ~10 m
136 above the ground level. It is an educational institute as well as residential campus having restaurants
137 nearby and very close to (<200 m) heavy traffic road. Lalchandani et al., (2021); Rai et al., (2020)
138 observed source signatures of emissions from industries, power plants, vehicles, and waste burning in this
139 site.

140 **2.1.2. Delhi NCR site 2: IITMD.**

141 Offline PM$_{2.5}$ sampling was carried out on the rooftop of the main building at the Indian Institute of
142 Tropical Meteorology Delhi (IITMD) (28.63°N, 77.167°E; ~220 m above msl) about 15 m above the
143 ground level. Moreover, HR-ToF-AMS and Xact ambient metal mass monitor were installed inside a

144 temperature-controlled laboratory on the 2nd floor of the same building at the height of ~8 m from the

145 ground level. This site is placed in the central urban area of Delhi and surrounded by Central Ridge

146 reserve forest and residential areas (Tobler et al., 2020) and around 14 km away in North West direction

147 from IITD. A recent study by Lalchandani et al. (2021) observed the site is dominated by emissions from

148 traffic, solid fuel burning, and oxidized organic aerosols. The location of the sampling sites are shown in

149 Fig. 1.

150 **2.2. Sampling details**

151 **2.2.1 Offline sampling**

152 Biweekly 24 hrs (January-May and August-September 2019) and daily 24 h (June-July and October-

153 December 2019) $PM_{2.5}$ samples were collected on quartz filter substrates (Whatman; 8×12 inches) using

154 a high-volume sampler (HVS) with a flow rate of 1.13 m^3/min. Blanks were collected in the field by

155 placing a fresh filter in the sampler while not running. A total of 64 filters (60 from IITD site during June-

156 July 2019 including 4 blanks) were collected in summer whereas, a total of 186 filters (90 from each site

157 during October-December 2019 plus 6 blanks) were collected in winter. The collected filters, including

158 field blanks, were zip-locked and stored in the freezer at each site and periodically transported to CESE

159 (Centre for Environmental Science and Engineering), IIT Kanpur, where they were further stored at -20˚C

160 in a deep freezer prior to analysis. For this study, the samples from the common period of offline and

161 online sampling (October-December 2019) from the two sites were analyzed for WSIS (SO_4^{2-}, NO_3^-, NH_4^+

162 and Cl^-) using an IC, and 32 metals (Al, Na, K, Ca, Ti, V, Cr, Mn, Fe, Ni, Cu, Zn, As, Se, Rb, Sr, Zr, Cd,

163 Sn, Sb, Ba, Pb, Cs, La, Ce, Pt, Tl, Mg, Li, Mo, Co and Pd) using an ICP-MS. More details of analytical

164 procedures are given in the instrumentation section.

165 **2.2.2 Online sampling**

166 At both IITD and IITMD site, high-resolution time-of-flight aerosol mass spectrometers (HR-ToF-AMS,

167 Aerodyne Research Inc., Billerica, MA) (Canagaratna et al., 2007; DeCarlo et al., 2006), equipped with

168 $PM_{2.5}$ aerodynamic lens (Peck et al., 2016) (Aerodyne Research Inc., Billerica, MA, USA) were installed

169 inside air-conditioned laboratories. Ambient fine particulate matters were sampled through $PM_{2.5}$ cyclone

170 (BGI, Mesa Labs. Inc.) inlet at IITD with a flow rate of 5 lpm (l/min) using a 2.44 m long stainless-steel

171 tubing (0.3 inch I.D and 0.4 inch O.D) and through black silicon tubing (0.19 inch I.D) at IITMD, placed

172 1.5 m above the rooftop. A Nafion dryer (MD-110-144P-4: Perma Pure, Halma, UK) was used to dry the

173 ambient aerosols to maintain the output RH at 20%. At IITD, data were collected from 12th October 2019-

174 31st December 2019 and 2nd June 2019-21st July 2019 during winter and summer campaigns respectively.

175 The data between 1st November and 14th November was not available, due to hardware issues in the AMS

176 during that period. At IITMD, data were only collected during winter campaign from 25th October 2019 to

177 31st December 2019.

178 Two Xact 625i ambient metal monitors (Cooper Environmental Services, Beaverton, Oregon, USA) were

179 installed inside temperature controlled laboratories at IITD and IITMD. Ambient aerosols were sampled

180 through a PM$_{2.5}$ inlet with a flow rate of 16.7 lpm. A separate sampling line of 2.44 meter (1.25 inch I.D)

181 for the Xact which was made of aluminium was installed. A heater was set up at the end of the sampling

182 line to ensure 45% RH set point. At IITD, sampling was carried out from 1st October 2019-31st December

183 2019 and 30th May 2019-25th July 2019 during the winter and summer campaign, respectively. However,

184 data between 16th July and 24th July were not available due to hardware breakdown. At IITMD, samples

185 were collected from 1st October 2019-31st December 2019 but data from 18th November to 26th

186 November 2019 and 30th November to 14th December 2019 were not available due to instrumental

187 problems.

188 Online measurements of inorganic ions (SO_4^{2-}, NO_3^-, NH_4^+ and Cl^-) from HR-ToF-AMS were compared

189 with the WSIS using an IC. Parallelly, heavy and trace metals obtained from Xact ambient metal mass

190 monitor were compared with the metal data from the offline filter measurements using an ICP-MS.

191 Though the sampling periods of AMS, Xact, and HVS were different for different seasons and different

192 sites as well (Table 1), only the common periods of online and offline sampling have been discussed in

193 this study for comparison.

194 Table 1. Sampling strategy and instrumentation used.

	Interval	IITD	IITMD
Quartz filter Sampling	3 days	January-May 2019	January-May 2019
		August-September 2019	August-September 2019
	24 hrs	June-July 2019	June-July 2019
		October-December 2019	October-December 2019
HR-Tof-AMS	2 mins	2nd June-21st July 2019	25th October-31st December 2019
		12nd October-31st December 2019	
Xact	30 mins	30th May-25th July 2019	1st October-31st December 2019
		1st October-31st December 2019	

195 Filters from the common periods were analysed for WSIS and heavy and trace metals using an IC and ICP-MS respectively.

2.3. Instrument details

2.3.1 WSIS measurements by IC and HR-ToF-AMS

For WSIS analysis, 9 sq.cm punch area of each collected filter was soaked in 30 ml of high purity milli-q water (resistivity-18.20 MΩ cm) for 12 hours in pre-cleaned borosilicate test tubes to ensure maximum solubility. The amount of water added, soaking time, etc. effect the solubility of the ions as well as the extent of extraction. Details can be found in our previous paper (Bhowmik et al., 2020). Soaked samples were filtered through 0.22 µm quartz filter papers to remove any suspended contaminations after an ultrasonication for 50 mins. Cl^-, NO_3^-, SO_4^{2-} and, NH_4^+ were measured for all the filter extracts by an IC (Metrohm 883 Basic IC plus for cations and 882 compact IC plus for anions). Separate columns for the analysis of cations and anions were installed in two separate modules. For anion and cation separation, an AS 5-250/4.0 chromatography column and C-6 column was used, respectively. The sample carried by 3.2 mM Na_2CO_3+1 mM $NaHCO_3$ solution and 2.7 mM HNO_3 solution in the anion and cation module separately passes through the charged columns to analyze each ion according to their polarity. The calibration was performed by a seven-point method with a range of standards prepared by the serial dilution from the stock solution standard of 10 ppm purchased from Metrohm. The uncertainty of the water-soluble inorganic ions measured by IC was estimated as 4% (coverage factor~2) by the approach described in Yardley et al. (2007).

HR-ToF-AMS measures size-resolved mass spectra of non-refractory particles (PM components that vaporize at 600°C and 10^{-5} Torr, e.g., organics, nitrate, sulphate, ammonium, and some chlorides) of submicron particulate matters. The details of this instrument can be found elsewhere (DeCarlo et al., 2006). Briefly, ambient aerosols are collected through an orifice of 100 μm diameter and focused into a narrow particle beam by an aerodynamic lens system installed inside the instrument, which has a transmission efficiency of > 50% for $PM_{2.5}$ (DeCarlo et al., 2006; Peck et al., 2016). The particle size is determined after analyzing the time of flight, i.e., time taken to travel along the length of the sizing chamber. The NR-PMs are then vaporized by hitting the vaporizer at 600°C and at a vacuum of 10^{-7} Torr. Further, the vaporized molecules are electronically ionized at 70 eV, followed by detection by a mass spectrometer as per their *m/z*. HR-ToF-AMS can be operated in W-mode or V-mode. For this study, it was operated in V-mode with a sampling time of 2 mins. Mass spectra (MS) mode, in which mass spectra of the components are measured, and particle time-of-flight (PToF) mode in which the size-resolved mass spectra are measured, are alternated in every 30s in 2 cycles. The HR-ToF-AMS was calibrated using standard protocols provided in our previous publication (Lalchandani et al., 2021; Singh et al., 2019).

To determine the mass concentration of NR-PMs, Unit mass resolution (UMR) analysis was done using the SQUIRREL data analysis toolkit (version 1.59) programmed in IGOR Pro 6.37 software (Wavemetrics, Inc., Portland, OR, USA). High resolution (HR) analysis was also done on the data set using Peak Integrated Key Analysis (PIKA version 1.19) toolkit. A recommended collection efficiency (CE) of 1 (Hu et al., 2017) was used for capture vaporizer. At the beginning and mid of each campaign at the two sites, ionization efficiency (IE) calibration was performed by injecting mono-disperse 300 nm ammonium nitrate and ammonium sulphate particles into AMS and a condensation particle counter (Jayne et al., 2000). A relative ionization efficiency (RIE) of 4.05 and 4.35 was used for IITD and IITMD site, respectively in case of NH_4. RIE of SO_4 was taken as 2.89 and 1.67 for IITD and IITMD, respectively. For Org and Cl, by default a RIE of 1.4 and 1.3 were taken, respectively. More details can be found in (Lalchandani et al., 2022).

2.3.2 Heavy and trace metal measurements by ICP-MS and Xact 625i

For the analysis of heavy and trace metals, 15 sq. cm area of each collected filter was digested in an acid mix of 0.5 ml HF+1.5 ml HNO_3 for 4 hours within closed HDPE Teflon tubes using a Hot plate (Savillex-HF resistive Model number 88888:00000). The temperature range should be ~90-120˚C to ensure complete digestion of the elements. Further, 2.5 ml of $HClO_4$ was added to the precipitates, left over the Teflon tube wall and the tubes were kept on the hot plate at 220-240˚C for another 4 hours with the lids open for complete evaporation of the acid mix. Moreover, the residual was dissolved in 6N HNO_3 and diluted with de-ionized water (resistivity-18.20 MΩ cm) followed by filtering through 0.22 μm quartz filter papers prior analysis. Details can be found in our forthcoming paper. This method is well established and used in many studies (Minguillón et al., 2012; Querol et al., 2008).

Thirty two metals (Al, Na, K, Ca, Ti, V, Cr, Mn, Fe, Ni, Cu, Zn, As, Se, Rb, Sr, Zr, Cd, Sn, Sb, Ba, Pb, Cs, La, Ce, Pt, Tl, Mg, Li, Mo, Co and Pd) were analyzed for all filter extracts using an ICP-MS (Thermo Scientific iCAP Q ICP-MS) at IIT Kanpur Environmental Engineering laboratory. Si could not be determined in the filter samples because Si is the primary constituent of the quartz filters and hence digested during sample preparation. Samples were first introduced to a nebulizer using an injector attached to an autosampler for transformation into fine aerosol droplets followed by ionization at a very high temperature (8000K) in Ar-plasma. The elements elute as per their *m/z*. A known concentration (5 ppb) of Ge was used as an internal standard to monitor the instrumental drift during the analysis. The overall average drift was reported as ± 10%. The calibration was performed by ten-point method with a range of mix standards prepared by the serial dilution from the High purity multi-element (35 elements) standards (soluble in 1% HNO_3, 100 ppm) purchased from Sigma Aldrich.

The Xact 625i Ambient Metals Monitor (Cooper Environmental Services (CES), Beaverton, OR, USA) uses X-ray fluorescence to measure the real-time elemental data in particulate matter. For this study, a $PM_{2.5}$ inlet was used. Details of the instrument can be found in Furger et al., 2017. Briefly, aerosol samples were collected on a Teflon filter tape followed by hitting the loaded area with X-rays and the fluorescence measured by a silicon drift detector (SDD). Thirty elements: Al, Si, S, Cl, K, Ca, Ti, Cr, Mn, Fe, Co, Ni, Cu, Zn, As, Se, Br, Rb, Sr, Zr, Mo, Cd, In, Sn, Sb, Te, Ba, Pb, Bi, and Bi were measured with 30 min time resolution. The Xact 625i was calibrated during each campaign using thin film standards for the individual elements. The reproducibility was observed within ± 5%. Every midnight energy alignment checks were performed for 15 mins (00:15 to 00:30) (for Cr, Pb, Cd and Nb). An uncertainty of ~10% was reported by the manufacturer in an interference free situation (USEPA & Etv, 2012). This included 1.73% from flow (CEN, 2014), 5% for standard reproducibility or uncertainty during calibration (USEPA, 1999) and 2.9% from term stability as reported in Tremper et al. (2018). More details on the instrumental set up and stability check during the summer and winter campaign can be found in Rai et al. (2020) and Shukla et al. (2021).

3. Results and discussions

3.1. Online and offline measurements of WSIS and their comparison

Large temporal variability was observed in both offline and online measurements of WSIS (NO_3^-, SO_4^{2-} and, NH_4^+ and Cl^-) during the winter campaign and summer campaign at both sites. The inorganics data with 2 mins interval from HR-ToF-AMS were averaged over the sampling period of the filters, i.e., 24 hours. The time series of NO_3^-, SO_4^{2-}, NH_4^+, and Cl^- during the summer and winter campaign at IITD and winter campaign at IITMD are shown in Fig. SM1 in the supplementary material. Higher peaks of inorganics were observed during 25th Oct-18th Nov during the winter campaign at IITD, which was the agricultural crop-residue burning period (Nagar et al., 2017). During the winter campaign, NO_3^- was the most abundant ion followed by SO_4^{2-}, NH_4^+ and Cl^- for both offline and online measurements at both the sites whereas, during the summer campaign at IITD, NO_3^- was the most abundant ion followed by NH_4^+, SO_4^{2-} and Cl^- in online measurement (HR-ToF-AMS). Similar results were observed in our companion paper, Shukla et al. (2021). Interestingly, in the case of offline measurements during the summer campaign at IITD, NO_3^- was least abundant, and the sequence changed as $SO_4^{2-} > NH_4^+ > Cl^- > NO_3^-$. The average concentrations with their ranges are tabulated in Table SM1 in supplementary material, and the mean, maximum and minimum concentration are shown in Fig. 2 using box plots.

Comparability and correlation between offline and online measurements were evaluated in this study by applying linear regression using offline data as the independent and online data as the dependent variable. The comparability of NH_4^+ measurements was observed to be good for both summer and winter campaigns at both sites. During the winter campaign, the correlations were $R^2=0.76$, and $R^2=0.89$, and the slopes were closer to 1 (0.99 for IITD and 0.93 for IITMD) for IITD and IITMD, respectively (Fig. 3). Interestingly during the summer campaign at IITD, though the correlation improves ($R^2=0.91$), the slope decreases to 0.49. This is likely because the vapor concentration of sulfuric acid (H_2SO_4) is higher during summers. As a result of which, the adsorption of sulfuric acid on PM deposited on the filter papers happens during summers which reacts with gaseous ammonia (NH_3) to form a relatively stable particulate $(NH_4)_2SO_4$ (Zhang et al., 2000), thus increasing ammonium concentration in the offline measurements during the warmer season, especially in the presence of dust (Nicolás et al., 2009).
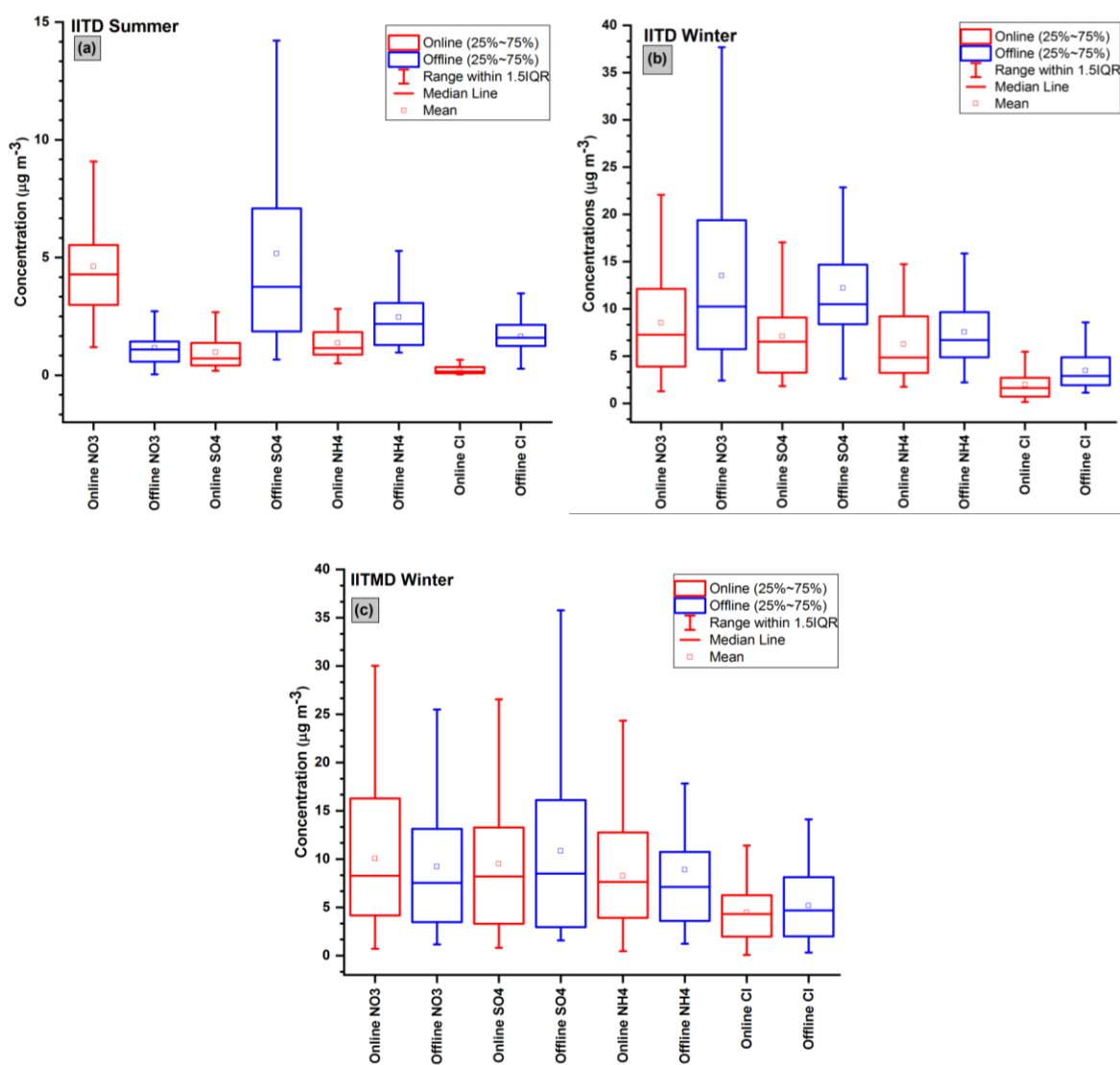
302   Fig.2. Box plots of online and offline measured secondary species (NO_3^-, SO_4^{2-} and, NH_4^+) and Cl^- during

303   (a) summer campaign at IITD, (b) winter campaign at IITD, and (c) winter campaign at IITMD site.

304   The filter-based measurements of SO_4^{2-} were higher than those from the online measurements for IITD

305   and IITMD during both the seasons (Fig. 2). Their comparability is characterized by a correlation

306   coefficient of $R^2=0.93$ with a slope of 0.17 and $R^2=0.82$ with a slope of 0.68 at IITD during the summer

307   and winter campaigns, respectively. Interestingly, offline SO_4^{2-} data correlates well with online SO_4^{2-} data

308   having a correlation coefficient of $R^2=0.93$ with a slope close to 1 (0.93) during the winter campaign at

309   IITMD (Fig. 3). A slope of less than 0.5 was observed in Malaguti et al., (2015) in Italy during the warm

310   period whereas the offline measurement of SO_4^{2-} was 34% lesser than the AMS measurements in Pandolfi

311   et al., (2014). The higher SO_4^{2-} concentrations on the un-denuded offline filter-based measurements could

312   be due to refractory sulfate (e.g., potassium or calcium sulfate). The higher filter-sulfate could also be

313   possibly because of the positive sampling artifact. The SO_2 is absorbed on the filter by the collected

314   alkaline particles (Nie et al., 2010). The higher concentration could also be due to the formation of

315   ammonium bi-sulfate or ammonium sulfate because of the reaction between gas-phase ammonia with the

316   acidic aerosols (Nicolás et al., 2009). Also, the un-denuded filter measurements could lead to higher

317   filter-sulfate. The interaction of gas phase ammonia with acidic aerosols can be minimized by using

318   denuders while collecting aerosols on the filters (Nault et al., 2020). Some studies suggested that the

319   organic sulfate, nitrate, and reduced nitrogen thermally decompose and/or under electron ionization in

320   AMS, producing inorganic ions. NO^+ and NO_2^+ contribute a significant fraction in organic nitrate (Day et

321   al., 2022) whereas, for organic sulfates, a large fraction of the signal contributes by SO^+, SO_2^+, and $SO_3^{\pm}$

322   (Chen et al., 2019). Though the additional inorganics are minimum, this could lead to possible marginal

323   biases between the online and offline measurement of the inorganics.~~Some studies suggested that the~~

324   ~~NH₄, SO₄ and, NO₃ measured by AMS have interferences from organics and can often be misinterpreted~~

325   ~~as fully inorganic (Chen et al., 2019; Farmer et al., 2010; Day et al., 2021). Though the interference is~~

326   ~~minimum, this could lead to possible biases between the online and offline measurement of the~~

327   ~~inorganics.~~

328

329

330
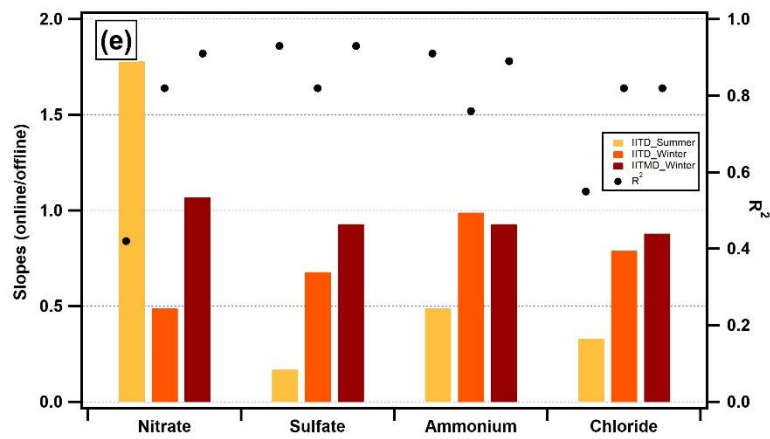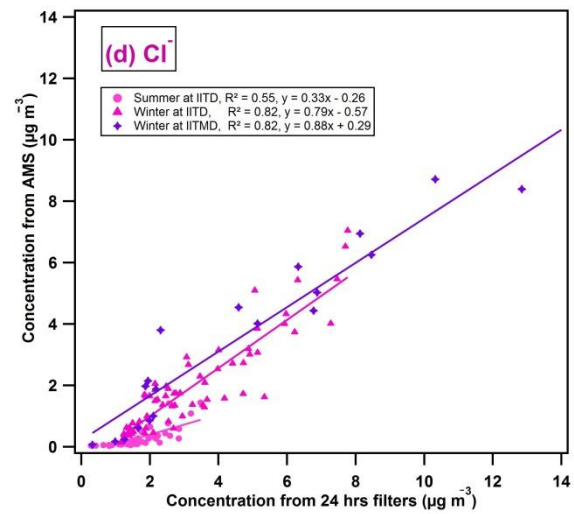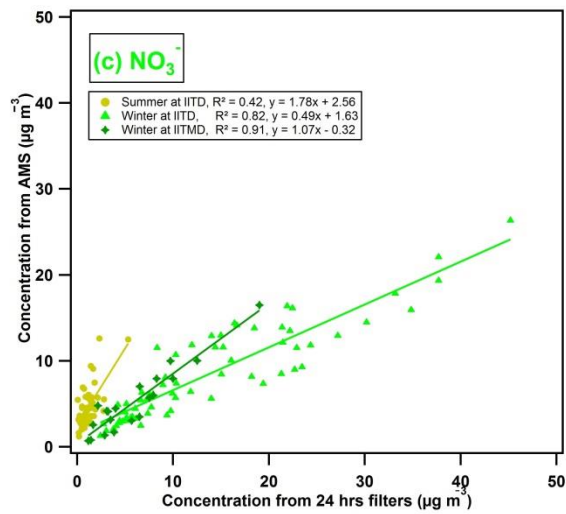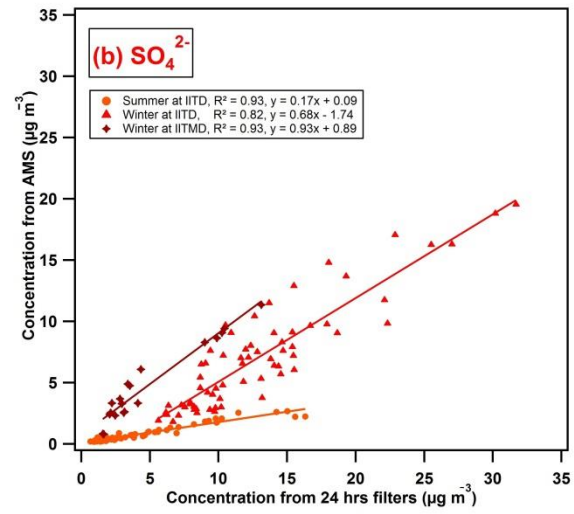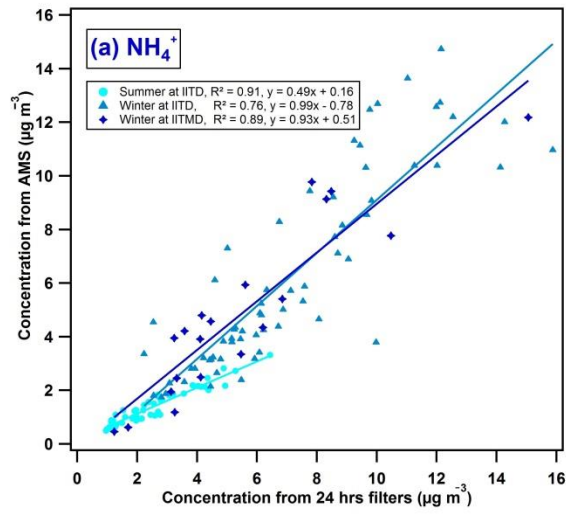
Fig.3. Scatter plots between online and offline measured (a) NH_4^+, (b) SO_4^{2-}, (c) NO_3^-, (d) Cl^- concentrations and (e) comparison of slopes (online/offline) and R^2 of the measured inorganic ions in $PM_{2.5}$ during summer and winter campaign at IITD and during winter campaign at IIITMD.

The online and offline NO_3^- measurements posed a good correlation during winter ($R^2 = 0.91$ and slope of 1.07 at IITMD, $R^2 = 0.82$ and slope of 0.49 at IITD) whereas the correlation worsens during summer at IITD ($R^2 = 0.42$ and slope of 1.78) (Fig. 3). The slopes and correlation coefficient for the WSIS are listed in Table 2. The NO_3^- concentrations measured by the HR-ToF-AMS were higher than the offline data during summer at IITD and during winter at IITMD whereas, filter-based measurements of NO_3^- were higher during winter at IITD (Fig. 2). The higher offline NO_3^- concentrations during winter at IITD can be possibly because of the positive artifact due to the absorption of gas-phase nitric acid (HNO_3) on the filter (Chow, 1995). Many studies (Chow et al., 2008; Kuokka et al., 2007; Malaguti et al., 2015) reported higher concentrations of NO_3^- from high time resolution measurements than filter-based measurements due to the evaporation of ammonium nitrate collected on filters over the duration of sample collection (Pakkanen & Hillamo, 2002; Schaap et al., 2004; Kuokka et al., 2007). Pandolfi et al. (2014) observed NO_3^-_ HR-AMS/Filter ratios of ~1.7 at Barcelona and Montseny in Europe. This evaporation loss increases with the decrease of humidity and the increase of temperature (Chow et al., 2008; Takahama et al., 2004). Also, complete evaporation may occur beyond 25°C (Schaap et al., 2004). Chow et al. (2008) observed the evaporation loss from quartz filter to be more than 80% during the warm season in central California. The high temperature (35°C-48°C) during the long sampling hours (24 hours) may be a possible reason for the poor correlation between online and offline NO_3^- measurements during the summer campaign at IITD. Schaap et al. (2004) reported that the NO_3^- volatilization during a 24-h sampling period not only depends on the sampling instruments and ambient conditions, but also on sampling strategy. If the sampling strategy is evening-to-evening (24 hours), the samples will lose the night NO_3^- sampled during the night with the increasing temperature during the day. However, during morning-to-morning sampling strategy, the filters will collect the night NO_3^- quantitatively throughout the night, but the higher temperature in the afternoon of the previous day may promote the loss of afternoon NO_3^- from the filters (Malaguti et al., 2015). If the sampling strategy is evening to evening (24 hours), the samples will lose the NO_3^- sampled during night with the increasing temperature during the day. However, during morning to morning sampling strategy, the filters will collect the NO_3^- quantitatively at night, and the higher temperature in the afternoon of the previous day may promote the loss of NO_3^- from the filter (Malaguti et al., 2015). In this study, the sampling time was from 6:30 am to the next day 6.30 am. Therefore, the filter-based inorganic measurements suffered from a negative sampling artifact due to

363 the evaporation of nitrate collected during the forenoon in a temperature of 20°C-25°C during the winter
364 campaign and ~ 38°C-45°C during the summer campaign.

365 Table 2. Regression coefficients and slopes for the comparison of WSIS measured by HR-ToF-AMS and
366 IC.

Sites	NO_3^-		SO_4^{2-}		NH_4^+		Cl^-	
	R^2	Slope	R^2	Slope	R^2	Slope	R^2	Slope
IITD Summer	0.42	1.78	0.93	0.17	0.91	0.49	0.55	0.33
IITD Winter	0.82	0.49	0.82	0.68	0.76	0.99	0.82	0.79
IITMD Winter	0.91	1.07	0.93	0.93	0.89	0.93	0.82	0.88

367 We observed higher Cl^- concentration in filter-based measurement than online measurement using HR-
368 ToF-AMS during both campaigns at IITD and winter at IITMD. A good correlation of R^2= 0.82 with a
369 slope of 0.79 and R^2= 0.82 with a slope of 0.88 was observed during the winter campaign at IITD and
370 IITMD, respectively (Fig. 3). Interestingly, during the summer campaign at IITD the comparability was
371 moderate with a correlation coefficient of R^2= 0.55 and a slope of 0.33. A correlation coefficient of R^2=
372 0.83 between Dp <10 μm measured with the MARGA and analyzed from Teflon filters was reported in
373 Makkonen et al., (2012) during Feb-May. Lower temperature and higher RH during winter retains Cl^- in
374 particulate phase for long enough to be detected which is not the case in summer. Further, Cl^- is
375 predominantly found in the coarse fraction. Also, while AMS only measures the NR-Cl^- (Manchanda et
376 al., 2021), e.g. NH_4Cl, which can vaporize at 600˚C but cannot measure Cl^- from refractory-KCl, IC
377 measures chloride from all the water-soluble chloride salts, including NH_4Cl and KCl. This probably
378 justifies the lower concentration of Cl^- in online measurement from AMS than filter-based measurements.
379 We also compared Cl^- measurements from Xact 625i with the measurements from IC. Interestingly, IC
380 measurements of Cl^- were found to be higher than Xact 625i measurements during summer at IITD and
381 winter at IITMD. The Cl measurements from Xact 625i were ~1.9 times higher than the measurements
382 from IC during winter at IITD (see fig. SM2 in supplementary material). The correlations were found to
383 be good during winter (R^2= 0.83 and 0.76 at IITD and IITMD respectively) and worsen during summer
384 (R^2= 0.27 at IITD), similar to what we observed for AMS_Cl^- and IC_Cl^-. It could be due to the
385 differences in water-soluble fraction of chloride in the samples, as ionic concentration (IC) represents
386 water-soluble fraction whereas elemental concentration (Xact 625i) represents total concentration. Also, a
387 lot particulate bound chloride in the atmosphere is in the form of ammonium chloride (Manchanda et al.,
388 2021). Part of the ammonium chloride collected during the day long offline sampling would have
389 vaporized, giving lower concentration from IC measurements. Further investigation is needed to draw a
390 firm conclusion.

3.2 Online and offline measurements of heavy and trace metals and their comparison

For the inter-comparison of heavy and trace metal concentrations from Xact 625i and ICP-MS, the half-hourly Xact 625i data were averaged to 24 hours filter sampling interval. A total of 32 elements were analyzed on each filter using ICP-MS while, 27 elements were measured in Xact 625i at IITD during summer and winter campaign, and 30 elements were measured in Xact 625i at IITMD during the winter campaign. The spatial and temporal variations of the crustal and trace elements are shown in Fig. SM3. Al and Ca concentrations were the most abundant in ICP-MS and Xact measurements respectively during the summer season (Fig. 4a, 5a & 5b) because of the increase in the crustal activities whereas K concentrations were significantly high for both the measurements during winter (Fig. 4d, 4g, 5c, 5d, 5e and 5f) due to mass-scale agricultural crop-residue burning in the adjoining states of Punjab and Haryana. Elements emitted from anthropogenic activities, e.g., coal-fired power plants (As, Se, Hg, Pb), traffic emissions (Cr, Pb, Mn), wear debris emission (Cu, Cd, Fe, Ga, Mn, Mo), etc. are found to be in higher concentration during winter campaign than summer campaign for both the measurements. Similar results were observed in our companion paper Shukla et al. (2021). The average values of metals along with their ranges are tabulated in Table SM2 and the statistics involved mean, upper, and lower values of some major elements are shown in Fig. 4. Box plots for rest of the metals can be found in Fig. SM4.

408
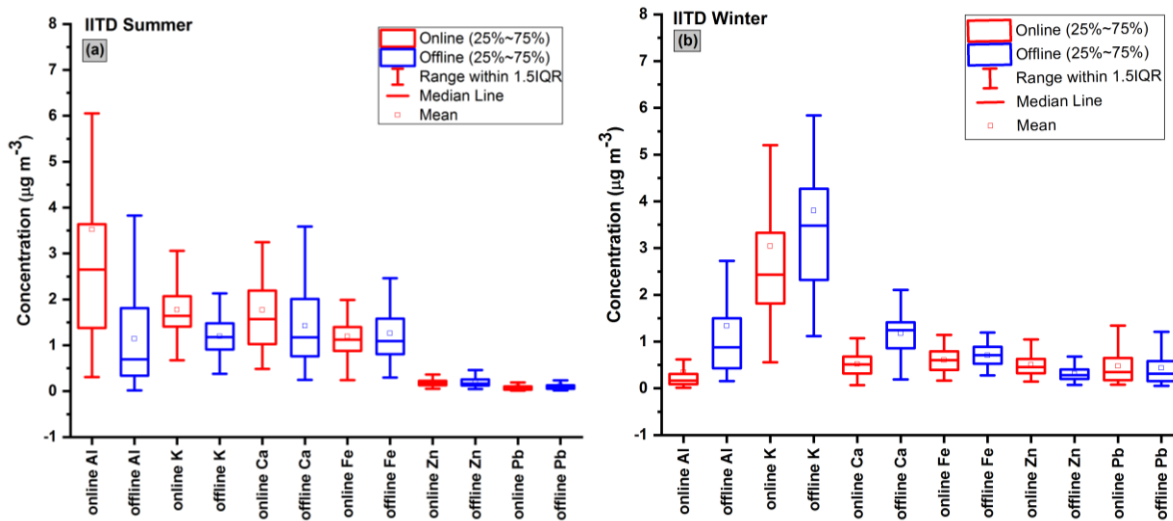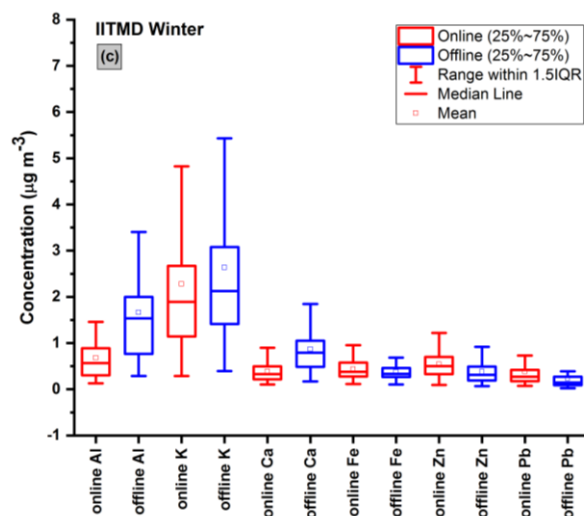
Fig.4. Box plots of some major elements measured offline and online during (a) summer campaign at IITD, (b) winter campaign at IITD, and (c) winter campaign at IITMD site. The box plots for rest of the heavy and trace elements are shown in fig. SM4 of the supplementary material.

The trends of the elemental concentration in decreasing order for both ICP-MS and Xact measurements during summer and winter at IITD and winter at IITMD are shown in Fig. SM5. The trace metals such as Cd, Mn, Mo, Ba, Pd etc. contribute a small portion in $PM_{2.5}$ in terms of their mass concentration but have a significant effect on human health. Fractions of elements in total element concentration for both the measurements during summer and winter campaign at IITD and during winter campaign at IITMD were shown in Fig. 5.

418

419

420
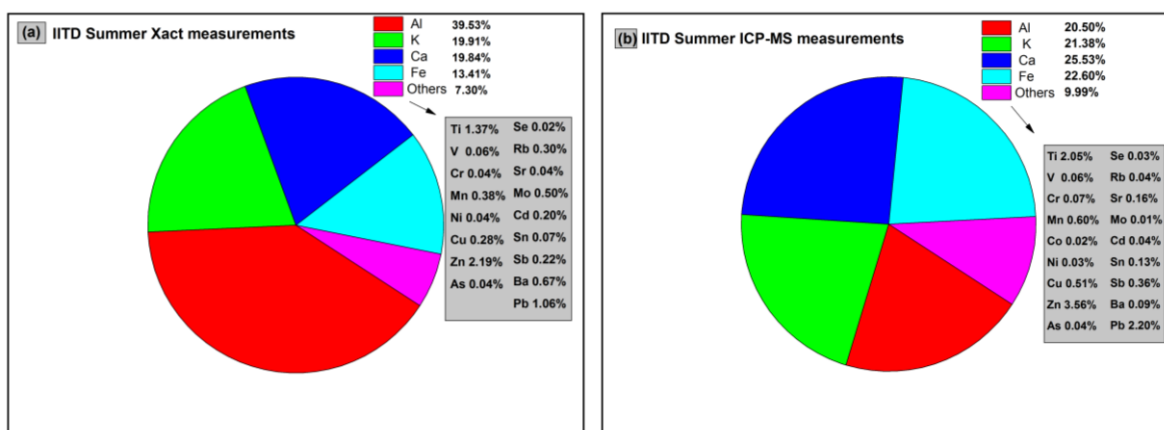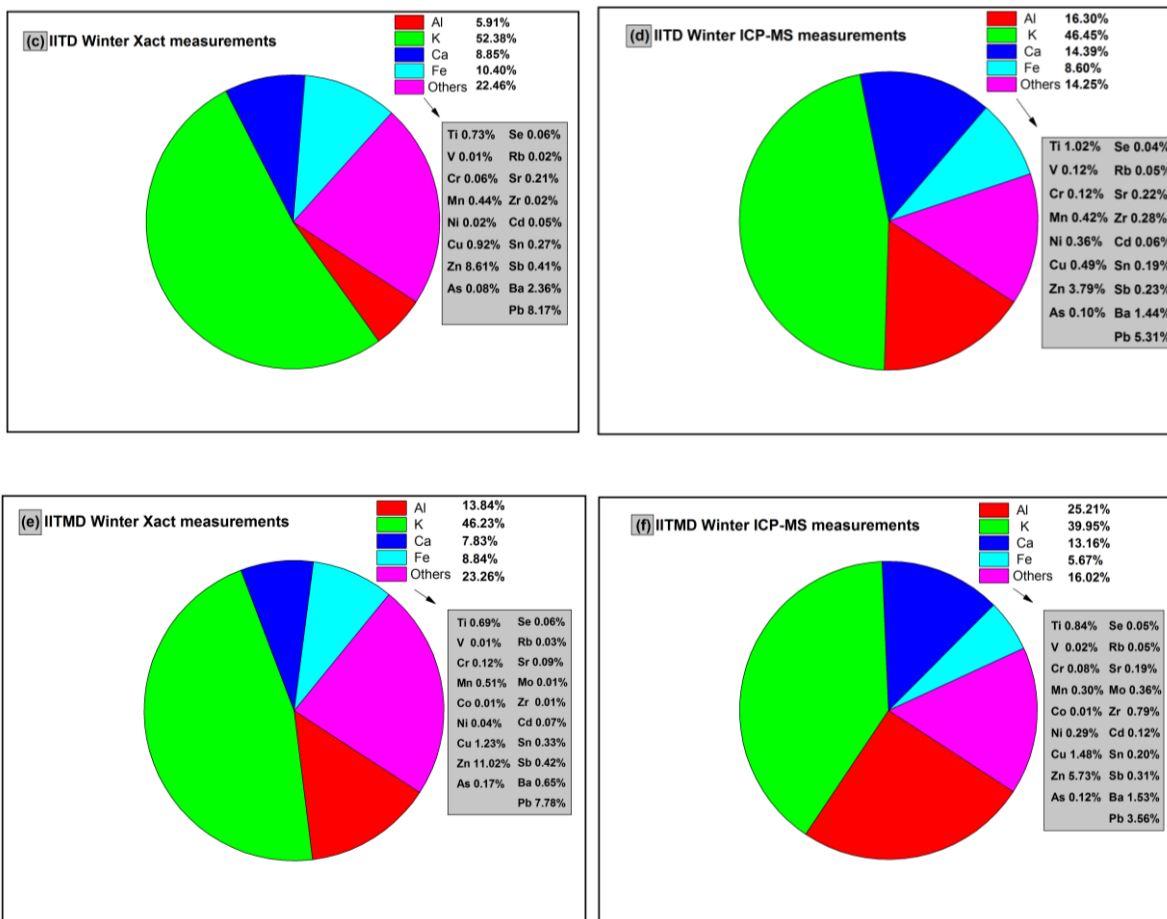
421   Fig.5. Fractions (%) of elements in total element concentration in PM$_{2.5}$ presented in pie format for online

422   (a,c,e) and offline (b,d,f) measurements during winter and summer at IITD and during winter at IITMD.

423   MDLs for ICP-MS measurements were calculated according to Escrig Vidal et al., (2009), and MDLs for

424   Xact 625i were obtained from the manufacturer. MDLs for the Xact 625i and ICP-MS are listed in Table

425   SM2 in the supplementary material. Though the half-hourly Xact data were averaged to 24 hours to the

426   corresponding interval of the filter sampling, for comparability check, MDLs of Xact 625i measurements

427   were taken for 30 mins sampling time while MDLs of filter-based elemental measurements were

428   calculated for 24 hours. Elements having data below $3 \times$ MDL were discarded from further examination

429   and unreliable as values below $3 \times$ MDL would lead to higher uncertainty (Furger et al., 2017). The

430   elements K, Ca, Ti, Mn, Fe, Ba, and Pb have >80% of their values above both offline and online MDLs,

431   and thus the data quality is reliable. Further, Ni, Mo, Zr have higher blank concentrations, and thus the

432   data is not reliable for ICP-MS measurements. The comparability of the elements measured online using

433   Xact 625i with those analysed using an ICP-MS, was checked for the common elements in these two

434   measurements (21 elements for IITD and 23 elements for IITMD) and is shown in Fig. 6.

435

436

437

438
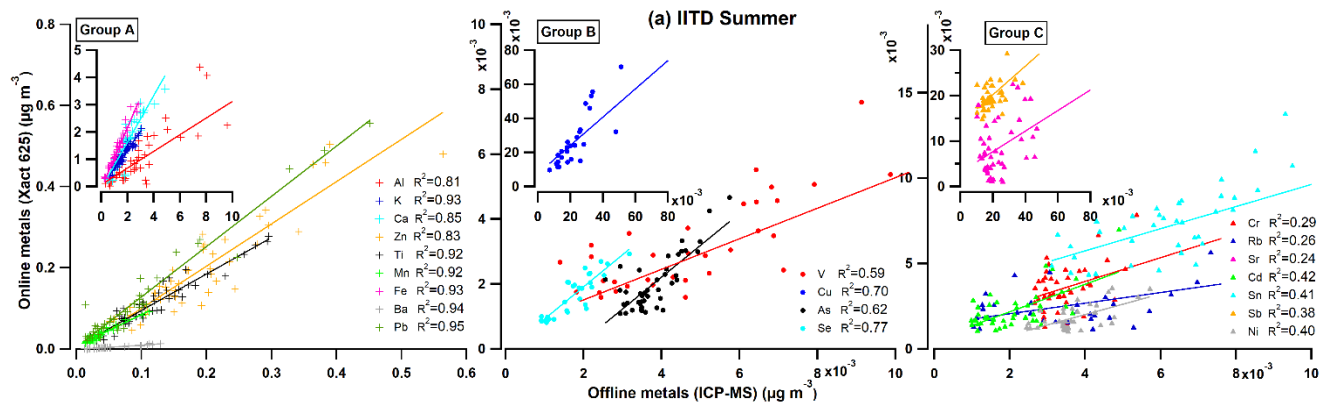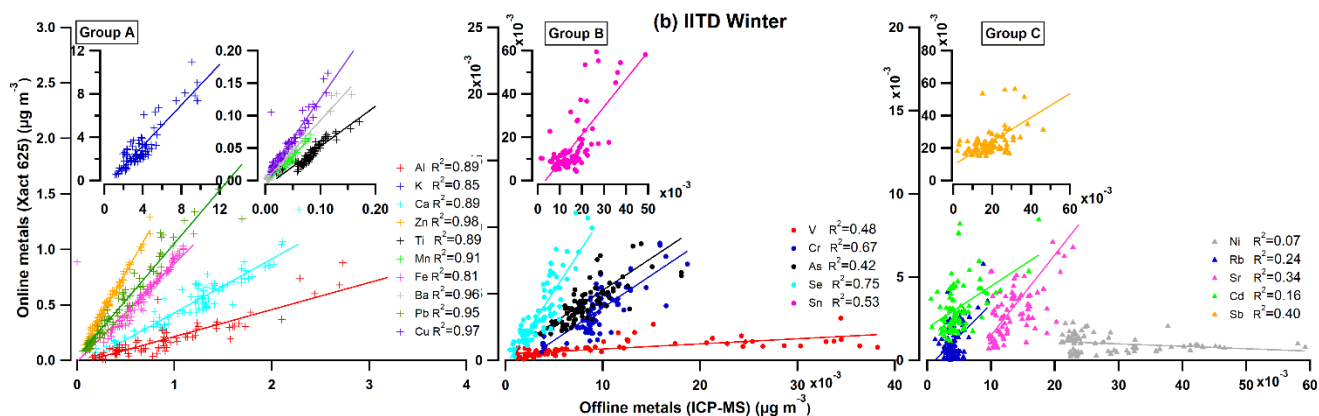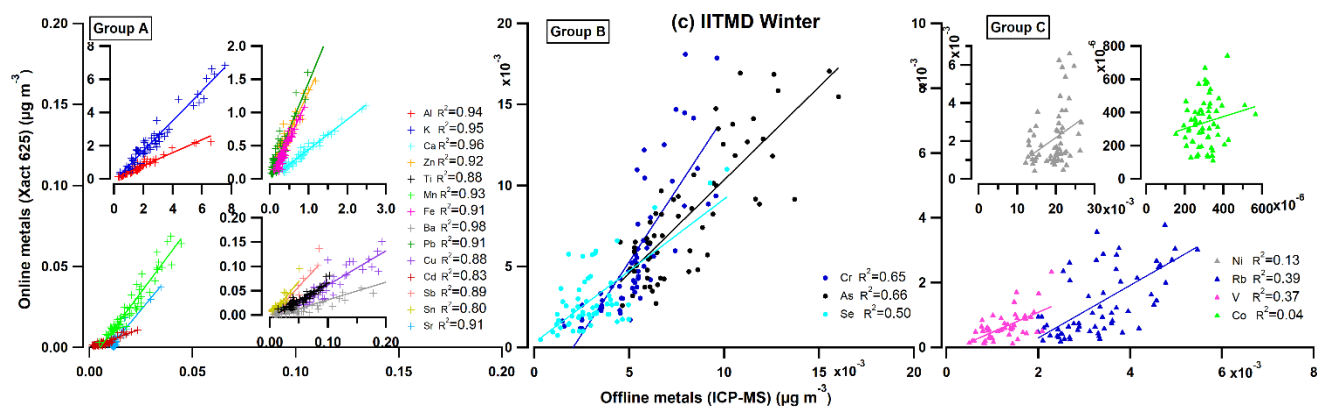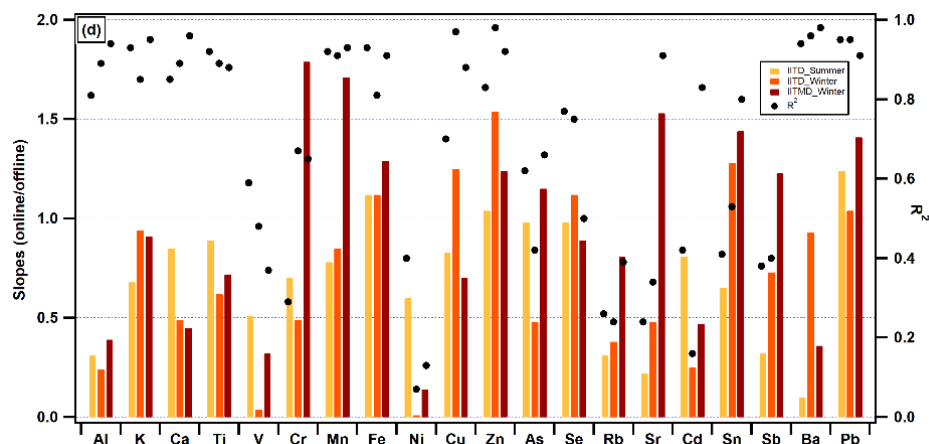
Fig. 6. Scatter plots and regression lines of Xact 625i vs. ICP-MS data for groups A, B, and C during (a) summer at IITD, (b) winter at IITD, (c) winter at IITMD, and (d) comparison of slopes (online/offline) & R^2 of the measured heavy and trace metals in $PM_{2.5}$ during the summer and winter campaign at IITD and winter campaign at IIITMD.

Based on their comparability characteristics, elements were grouped under 3 categories. Group A showed excellent linearity between the two methods with a correlation coefficient of $R^2 > 0.8$. Overall, group A consists of Al, K, Ca, Ti, Mn, Fe, Cu, Zn, Ba, and Pb during winter at IITD whereas, Cu showed in another group during summer at IITD. Though Sr, Cd, Sn, Sb had average values below MDLs and posed a lower correlation coefficient at IITD, interestingly, Sr, Cd, Sn, and Sb joined group A during winter at IITMD. To distinguish the potential difference in accuracy between the two methods, intercepts were not forced to be zero. The slopes are important, which indicate biases between the two measurements. The slopes of Zn, Fe, and Pb were closer to unity during summer at IITD (Fig. 6). K, Fe, Cu, Zn, Ba, and Pb achieved a slope of 0.94-1.25 during winter at IITD whereas, Mn, Fe, Zn, Pb, Sr, Sn, and Sb pose a slope slightly higher than unity during winter at IITMD (Fig. 6). A slight difference in cut-off value for the particle size can reduce the slopes from unity and produce ~10% difference in collected mass (Panteliadis et al., 2012). The slopes and the correlation coefficients are listed in Table 3.

In a comparison study conducted by USEPA & Etv. (2012) between Xact 625i and ICP-MS measurements, Ca, Cu, Mn, Pb, Se, and Zn were highly correlated except Cu. Cu was close to the MDL values of ICP-MS and Xact 625i. A good agreement was observed between Xact 625i and offline measurements using ED-XRF in South Korea by Park et al., (2014). The comparability between Xact measurements and ICP-MS measurements was checked for the elements As, Ba, Ca, Cr, Cu, Fe, K, Mn, Ni, Pb, Se, Sr, Ti, V, and Zn in Tremper et al. (2018). They observed an average R^2 of 0.93 and a slope of 1.07 for these elements. In the study by Furger et al., (2017) during a warmer season in Switzerland, an

462 excellent correlation ($R^2 > 0.95$) was found for Xact and ICP-OES/MS measurements of S, K, Ca, Ti, Mn,

463 Fe, Cu, Zn, Ba, and Pb. However, they found that the elemental measurements by Xact 625i were 28%

464 higher than ICP-OES/MS measurements for these 10 elements. In our study, Xact measurements of Fe,

465 Cu, Zn, and Pb yielded an average of 24% higher mass concentrations than ICP-MS measurements for

466 Group A elements during winter at IITD. Xact measurements were systematically 10% (average) higher

467 than ICP for Zn, Fe, and Pb during summer at IITD, whereas; we obtained an average of 41% higher

468 Xact measurements than ICP for Mn, Fe, Zn, Pb, Sr, Sn, and Sb during winter at IITMD in Group A

469 elements.

470 Group B was characterized by moderate linearity having $R^2 \sim 0.4$-0.8 and consisted of the elements V, Cu,

471 As, and Se during summer at IITD; V, Cr, As, Se, Sn during winter at IITD and Cr, As and Se during

472 winter at IITMD. These elements in Group B had their values very close to or below MDLs of at least

473 one of the analysis methods. During winter at both sites, Cr and As from ICP-MS have ~50-65% of their

474 values below MDLs, whereas ~68-72% of their values were above the MDLs of Xact 625i. Though some

475 of the elements in this group in different seasons have slopes near or greater than unity (see Table 3) like

476 Group A, their comparison is not statistically feasible.

477 Table 3. Regression coefficients and slopes for the comparison of Xact 625i and ICP-MS measurements.

Sites	Group A	Slope	R^2	Group B	Slope	R^2	Group C	Slope	R^2
	Al	0.31	0.81	V	0.51	0.59	Cr	0.7	0.29
	K	0.68	0.93	Cu	0.83	0.70	Co	-	-
	Ca	0.85	0.85	As	0.98	0.62	Rb	0.31	0.26
	Zn	1.04	0.83	Se	0.98	0.77	Sr	0.22	0.24
IITD Summer	Ba	0.1	0.94				Mo	-	-
	Ti	0.89	0.92				Cd	0.81	0.42
	Mn	0.78	0.92				Sn	0.65	0.41
	Fe	1.12	0.93				Sb	0.32	0.38
	Pb	1.24	0.95				Ni	0.6	0.4
	Al	0.24	0.89	V	0.04	0.48	Ni	0.01	0.07
	K	0.94	0.85	Cr	0.49	0.67	Rb	0.38	0.24
	Ca	0.49	0.89	As	0.48	0.42	Sr	0.48	0.34
IITD Winter	Ti	0.62	0.89	Se	1.12	0.75	Zr	-	-
	Mn	0.85	0.91	Sn	1.28	0.53	Cd	0.25	0.16

	Fe	1.12	0.81				Sb	0.73	0.40
	Cu	1.25	0.97						
	Zn	1.54	0.98						
	Ba	0.93	0.96						
	Pb	1.04	0.95						
	Al	0.39	0.94	Cr	1.79	0.65	Ni	0.14	0.13
	K	0.91	0.95	As	1.15	0.66	Rb	0.81	0.39
	Ca	0.45	0.96	Se	0.89	0.5	Mo	-	-
	Ti	0.72	0.88				Zr	-	-
	Mn	1.71	0.93				V	0.32	0.37
	Fe	1.29	0.91				Co	0.36	0.04
	Cu	0.70	0.88						
IITMD Winter	Zn	1.24	0.92						
	Ba	0.36	0.98						
	Pb	1.41	0.91						
	Sr	1.53	0.91						
	Cd	0.47	0.83						
	Sn	1.44	0.8						
	Sb	1.23	0.89						

478 The Group C elements, e.g., Ni, Rb, Sr, Zr, Cd, and Sb during summer at IITD; Cr, Co, Rb, Sr, Mo, Cd,
479 Sn, Sb, and Ni during winter at IITD and, Ni, Rb, Mo, Zr, V, and Co during winter at IITMD are
480 characterized by their bad correlation (R^2<0.4). Interestingly, measurements of some element e.g. Mo
481 during summer and winter at IITD and IITMD respectively, Co during summer at IITD, and Zr during
482 winter at both sites from both the methods did not correlate at all. For most of the elements in this group,
483 70-85% of measurements were below both method's MDLs and rest of the data were below 3 × MDLs.
484 The high and variable blank concentrations of these elements increased the MDL values in ICP-MS
485 measurement. The particle size dependent self-absorption effect and line interference between different
486 elements in Xact measurement could also increase the MDL values (Furger et al., 2017). This is probably
487 the reason for the values lower than MDLs for the elements in this group.

488 Overall, we observed 10-40% higher Xact measurements than ICP for some of the elements in Group A
489 during different seasons. The difference in the Xact and High-volume sampler inlet location and their
490 distance from the road can cause such difference in measurements (Furger et al., 2017). In the case of dust

491 resuspension from vehicular traffic, the number concentration of finer particulate matter tends to decrease
492 sharply within an increment of just 50m from the roadway (Hagler et al., 2009). In this study, we tried to
493 co-locate the two sample inlets, but it could not be avoided. Also, IITD and IITMD are both very close
494 (<200 m) to a roadway with moderate to heavy-duty traffic. The differences in online and offline
495 measurements may indicate a gradient in some elements due to very close proximity to heavy-duty traffic.
496 Also, the different temperatures of the sample inlets may give rise to a difference in measured
497 concentrations from both methods (Tremper et al., 2018). In this study, the blank corrected ICP-MS
498 measurements may result in overestimation or underestimation due to variable and high blank
499 concentration. The difference can also occur due to the digestion recovery rate for the digestion protocol
500 used for the filter analysis. Moreover, if the ambient elemental concentration is much lower than the
501 standards used for calibration of Xact, such differences may occur (Indresand et al., 2013).

502 **4. Conclusion**

503 Atmospheric WSIS (NO_3^-, SO_4^{2-}, NH_4^+, Cl^-) and heavy and trace elements in $PM_{2.5}$ were measured using
504 offline methods (IC for WSIS and ICP-MS for elements) and online methods (HR-ToF-AMS for
505 inorganics and Xact 625i for elements). These measurements were compared to assess the measurement
506 quality and sampling artifacts of these measurement techniques in the heavily polluted Delhi-NCR for
507 two different metrological conditions (winter and summer season). Field campaigns were conducted at
508 two NCR sites, namely, IITD during June-July 2019 and Oct-Dec 2019 and at IITMD during Oct-Dec
509 2019. The key findings of this study are summarized below.

510 • NH_4^+ concentrations from the IC and HR-ToF-AMS, compared well during winter with a slope
511   of 0.99 at IITD and 0.93 at IITMD. Interestingly, NH_4^+ concentrations were higher in offline
512   measurements during summer at IITD. The decrease in slope was probably due to the formation
513   of particulate $(NH_4)_2SO_4$.
514 • Offline SO_4^{2-} measurements were higher (with a slope of 0.17 during summer at IITD and 0.8
515   and 0.93 during winter at IITD and IITMD, respectively) during both seasons at both the sites
516   due to the positive sampling artifact. The absorption of SO_2 and the oxidation or condensation
517   process may result in additional sulphate.
518 • Lower NO_3^- concentrations (with a slope of 1.78 during summer at IITD and 1.07 during winter
519   at IITMD) were observed in the offline measurement during summer at IITD and during winter
520   at IITMD because of the evaporation of NH_4NO_3 from the filter substrates.   The evaporative
521   loss of nitrate from the filters was minimal in winter at IITMD. It aggravated during summer at
522   IITD due to the evaporation of ammonium nitrate in such a high temperature (35˚C-48˚C) range.

523   The higher NO_3^- concentrations (slope~0.49) in the filters than HR-ToF-AMS measurements
524   during winter at IITD can be due to the absorption of gas-phase HNO_3 on the filter.

525   • Offline Cl^- was consistently higher (with a slope of 0.33 during summer at IITD and 0.79 and
526   0.88 during winter at IITD and IITMD, respectively) than HR-ToF-AMS measurements during
527   both seasons at both sites mainly because HR-ToF-AMS only measures the NR-Cl^- whereas, the
528   offline Cl^- measurements includes chloride from all the water-soluble chloride salts. The
529   comparability degrades during summer due to the volatile nature of Cl^- in higher temperatures
530   and lower RH.

531   • The elements were grouped into three categories (Group A, B and C) according to their
532   comparability characteristics. The elemental data from Xact 625i were highly correlated
533   ($R^2>0.8$) with ICP-MS measurements of the 24 hr filters for Group A elements (Al, K, Ca, Ti,
534   Zn, Mn, Fe, Ba, and Pb). The Cu also showed up in this group during winter at IITD. About
535   80% of the data for these elements were above MDLs for both the methods. Though Sn, Sb, and
536   Cd had values below MDLs of one or both the methods, interestingly, they were highly
537   correlated ($R^2>0.8$) and, slopes are very close to unity for Sn and Sb during winter at IITMD.
538   The correlation coefficients > 0.8 for the elements in Group A indicated the high precision of
539   the online and offline measurements. Hence, these elements from any of these methods can be
540   reliably used for modelling studies.

541   • The elements under Group B had their values closer to or below at least one of the method's
542   MDLs. Cr and As had ~50-65% of their values below ICP-MS MDLs from ICP-MS, whereas
543   ~68-72% of their values were above Xact 625i MDLs during winter at both sites.

544   • Elements like Ni, Mo, and Zr measured from ICP-MS were not reliable due to their higher and
545   variable blank concentrations. No conclusion on their measurement accuracy by the two
546   methods can be drawn.

547   • In summary, the daily averaged half-hourly Xact 625i measurements were 10-40% higher than
548   24 hr filter measurements by ICP-MS depending upon the seasons, sites and elements in Group
549   A. Distance between two inlets for the two methods, distance of the inlets from the roadway,
550   line interference between two elements in Xact measurements, particle size, sampling strategy,
551   filter type, higher and variable concentrations in blank filters and digestion protocol for ICP
552   measurements can cause the difference in measurements between the two methods.

553 The above findings highlight the measurement methods' accuracy and implement the particular type of
554 measurements as needed. Denuders could be effective in avoiding the overestimation problems of
555 ammonium and sulphate in filter measurements and improve the comparison. Also, teflon filters instead

556   of quartz filters in the un-denuded sampler are reported to give better comparison for sulphate. The MDLs
557   in the Xact 625 measurements are higher than the MDLs for the offline method. Depending on the
558   objective of the campaign, Xact 625 can be deployed for a longer time interval to analyse the elements
559   that are below their MDLs. The high resolution real-time monitoring of non-refractory organics,
560   inorganics by HR-ToF-AMS and elements by Xact comes at the cost of high sensitivity in MDLs,
561   calibrations and cost. Whereas, cost effectiveness of conventional samplers makes it practical to deploy in
562   larger numbers at multi-sites simultaneously. Overall, high resolution real time sampling provides a rich
563   dataset for high and small pollution episodes. Future work should involve using different filter substrates
564   and different digestion protocols to re-evaluate the difference between these online and offline methods.
565   Although this study compares the PM species, a comparison of full source apportionment analysis
566   between online and offline methods should be done for more qualitative and quantitative insights.

567   **Author contribution**

568   HSB performed the offline analysis, data processing and wrote the manuscript. JD collected the AMS
569   data at IITD. AS and VL carried out the Xact and AMS data collection and processing respectively. NR,
570   MK, VS and SNT were involved with the supervision and conceptualization. All co-authors contributed
571   to the paper discussion and revision.

572   **Declaration of interests**

573   The authors declare that they have no conflict of interest.

574   **Acknowledgements**

575   The authors are thankful to Naba Hazarika and Mohd Faisal for collecting the Xact data at IITMD and
576   Pawan Vats for the sampling and collection of the filters at IITD. The authors are also thankful to Amit
577   Vishwakarma, Vaibhav Shrivastava and Harishankar for helping in offline analysis. This work is
578   financially supported by the Department of Biotechnology, Government of India (Grant No.
579   BT/IN/UK/APHH/41/KB/2016-17 dated 19th July 2017) and Central Pollution Control Board (CPCB),
580   Government of India to conduct this research under grant no. AQM/Source apportionment_EPC
581   Project/2017 dated 12th February 2019.

582   **Reference**

583   Bhowmik, H. S., Naresh, S., Bhattu, D., Rastogi, N., Prévôt, A. S. H., & Tripathi, S. N. (2020). Temporal and spatial

584 variability of carbonaceous species (EC; OC; WSOC and SOA) in PM2.5 aerosol over five sites of Indo-

585 Gangetic Plain. *Atmospheric Pollution Research*, *12*(June 2020), 375–390.

586 https://doi.org/10.1016/j.apr.2020.09.019

587 Chen, Y., Xu, L., Humphry, T., Hettiyadura, A. P. S., Ovadnevaite, J., Huang, S., Poulain, L., Schroder, J. C.,

588 Campuzano-Jost, P., Jimenez, J. L., Herrmann, H., O'Dowd, C., Stone, E. A., & Ng, N. L. (2019). Response

589 of the Aerodyne Aerosol Mass Spectrometer to Inorganic Sulfates and Organosulfur Compounds:

590 Applications in Field and Laboratory Measurements. *Environmental Science and Technology*, *53*(9), 5176–

591 5186. https://doi.org/10.1021/acs.est.9b00884

592 Chow, J. C. (1995). Measurement methods to determine compliance with ambient air quality standards for

593 suspended particles. *Journal of the Air and Waste Management Association*, *45*(5), 320–382.

594 https://doi.org/10.1080/10473289.1995.10467369

595 Chow, J. C., Watson, J. G., Lowenthal, D. H., Park, K., Doraiswamy, P., Bowers, K., & Bode, R. (2008).

596 Continuous and filter-based measurements of PM2.5 nitrate and sulfate at the Fresno Supersite. *Environmental*

597 *Monitoring and Assessment*, *144*(1–3), 179–189. https://doi.org/10.1007/s10661-007-9987-5

598 Day, D., Campuzano-Jost, P., Nault, B., Palm, B., Hu, W., Guo, H., Wooldridge, P., Cohen, R., Docherty, K.,

599 Huffman, J. A., de Sá, S., Martin, S., & Jimenez, J. (2021). A Systematic Re-evaluation of Methods for

600 Quantification of Bulk Particle-phase Organic Nitrates Using Real-time Aerosol Mass Spectrometry.

601 *Atmospheric Measurement Techniques Discussions*, *2*(3), 1–35. https://doi.org/10.5194/amt-2021-263

602 DeCarlo, P. F., Kimmel, J. R., Trimborn, A., Northway, M. J., Jayne, J. T., Aiken, A. C., Gonin, M., Fuhrer, K.,

603 Horvath, T., Docherty, K. S., Worsnop, D. R., & Jimenez, J. L. (2006). Field-deployable, high-resolution,

604 time-of-flight aerosol mass spectrometer. *Analytical Chemistry*, *78*(24), 8281–8289.

605 https://doi.org/10.1021/ac061249n

606 Escrig Vidal, A., Monfort, E., Celades, I., Querol, X., Amato, F., Minguillón, M. C., & Hopke, P. K. (2009).

607 Application of optimally scaled target factor analysis for assessing source contribution of ambient PM10.

608 *Journal of the Air and Waste Management Association*, *59*(11), 1296–1307. https://doi.org/10.3155/1047-

609 3289.59.11.1296

610 ~~Farmer, D. K., Matsunaga, A., Docherty, K. S., Surratt, J. D., Seinfeld, J. H., Ziemann, P. J., & Jimenez, J. L.~~

611 ~~(2010). Response of an aerosol mass spectrometer to organonitrates and organosulfates and implications for~~

612 ~~atmospheric chemistry. *Proceedings of the National Academy of Sciences of the United States of America*,~~

613 ~~*107*(15), 6670–6675. https://doi.org/10.1073/pnas.0912340107~~

614 Furger, M., Minguillón, M. C., Yadav, V., Slowik, J. G., Hüglin, C., Fröhlich, R., Petterson, K., Baltensperger, U.,

615 & Prévôt, A. S. H. (2017). Elemental composition of ambient aerosols measured with high temporal resolution

616 using an online XRF spectrometer. *Atmospheric Measurement Techniques*, *10*(6), 2061–2076.

617   https://doi.org/10.5194/amt-10-2061-2017

618   Gani, S., Bhandari, S., Seraj, S., Wang, D. S., Patel, K., Soni, P., Arub, Z., Habib, G., Hildebrandt Ruiz, L., & Apte,
619   J. S. (2019). Submicron aerosol composition in the world's most polluted megacity: The Delhi Aerosol
620   Supersite study. *Atmospheric Chemistry and Physics*, *19*(10), 6843–6859. https://doi.org/10.5194/acp-19-
621   6843-2019

622   Hagler, G. S. W., Baldauf, R. W., Thoma, E. D., Long, T. R., Snow, R. F., Kinsey, J. S., Oudejans, L., & Gullett, B.
623   K. (2009). Ultrafine particles near a major roadway in Raleigh, North Carolina: Downwind attenuation and
624   correlation with traffic-related pollutants. *Atmospheric Environment*, *43*(6), 1229–1234.
625   https://doi.org/10.1016/j.atmosenv.2008.11.024

626   Hong, C., Zhang, Q., Zhang, Y., Davis, S. J., Tong, D., Zheng, Y., Liu, Z., Guan, D., He, K., & Schellnhuber, H. J.
627   (2019). Impacts of climate change on future air quality and human health in China. *Proceedings of the*
628   *National Academy of Sciences of the United States of America*, *116*(35), 17193–17200.
629   https://doi.org/10.1073/pnas.1812881116

630   Hu, W., Campuzano-Jost, P., Day, D. A., Croteau, P., Canagaratna, M. R., Jayne, J. T., Worsnop, D. R., & Jimenez,
631   J. L. (2017). Evaluation of the new capture vaporizer for aerosol mass spectrometers (AMS) through field
632   studies of inorganic species. *Aerosol Science and Technology*, *51*(6), 735–754.
633   https://doi.org/10.1080/02786826.2017.1296104

634   Indresand, H., White, W. H., Trzepla, K., & Dillner, A. M. (2013). Preparation of sulfur reference materials that
635   reproduce atmospheric particulate matter sample characteristics for XRF calibration. *X-Ray Spectrometry*,
636   *42*(5), 359–367. https://doi.org/10.1002/xrs.2456

637   Jayne, J. T., Leard, D. C., Zhang, X., Davidovits, P., Smith, K. A., Kolb, C. E., & Worsnop, D. R. (2000).
638   Development of an aerosol mass spectrometer for size and composition analysis of submicron particles. In
639   *Aerosol Science and Technology* (Vol. 33, Issues 1–2, pp. 49–70). https://doi.org/10.1080/027868200410840

640   Jimenez, J. L., Jayne, J. T., Shi, Q., Kolb, C. E., Worsnop, D. R., Yourshaw, I., Seinfeld, J. H., Flagan, R. C., Zhang,
641   X., Smith, K. A., Morris, J. W., & Davidovits, P. (2003). Ambient aerosol sampling using the Aerodyne
642   aerosol mass spectrometer. *Journal of Geophysical Research: Atmospheres*, *108*(7).
643   https://doi.org/10.1029/2001jd001213

644   Lalchandani, V., Srivastava, D., Dave, J., Mishra, S., Tripathi, N., Shukla, A. K., Sahu, R., Thamban, N. M.,
645   Gaddamidi, S., Dixit, K., Ganguly, D., Tiwari, S., Srivastava, A. K., Sahu, L., Rastogi, N., Gargava, P., &
646   Tripathi, S. N. (2022). Effect of Biomass Burning on PM2.5 Composition and Secondary Aerosol Formation
647   During Post-Monsoon and Winter Haze Episodes in Delhi. *Journal of Geophysical Research: Atmospheres*,
648   *127*(1), 1–21. https://doi.org/10.1029/2021JD035232

649 Lalchandani, Vipul, Kumar, V., Tobler, A., M. Thamban, N., Mishra, S., Slowik, J. G., Bhattu, D., Rai, P., Satish,
650   R., Ganguly, D., Tiwari, S., Rastogi, N., Tiwari, S., Močnik, G., Prévôt, A. S. H., & Tripathi, S. N. (2021).
651   Real-time characterization and source apportionment of fine particulate matter in the Delhi megacity area
652   during late winter. *Science of the Total Environment*, *770*. https://doi.org/10.1016/j.scitotenv.2021.145324

653 Lipfert, F. W. (1994). Filter artifacts associated with particulate measurements: Recent evidence and effects on
654   statistical relationships. *Atmospheric Environment*, *28*(20), 3233–3249. https://doi.org/10.1016/1352-
655   2310(94)00167-J

656 Makkonen, U., Virkkula, A., Mäntykenttä, J., Hakola, H., Keronen, P., Vakkari, V., & Aalto, P. P. (2012). Semi-
657   continuous gas and inorganic aerosol measurements at a Finnish urban site: Comparisons with filters, nitrogen
658   in aerosol and gas phases, and aerosol acidity. *Atmospheric Chemistry and Physics*, *12*(12), 5617–5631.
659   https://doi.org/10.5194/acp-12-5617-2012

660 Malaguti, A., Mircea, M., La Torretta, T. M. G., Telloli, C., Petralia, E., Stracquadanio, M., & Berico, M. (2015).
661   Comparison of online and offline methods for measuring fine secondary inorganic ions and carbonaceous
662   aerosols in the central mediterranean area. *Aerosol and Air Quality Research*, *15*(7), 2641–2653.
663   https://doi.org/10.4209/aaqr.2015.04.0240

664 Manchanda, C., Kumar, M., Singh, V., Faisal, M., Hazarika, N., Shukla, A., Lalchandani, V., Goel, V., Thamban,
665   N., Ganguly, D., & Tripathi, S. N. (2021). Variation in chemical composition and sources of PM2.5 during the
666   COVID-19 lockdown in Delhi. *Environment International*, *153*(December 2020), 106541.
667   https://doi.org/10.1016/j.envint.2021.106541

668 Minguillón, M. C., Querol, X., Baltensperger, U., & Prévôt, A. S. H. (2012). Fine and coarse PM composition and
669   sources in rural and urban sites in Switzerland: Local or regional pollution? *Science of the Total Environment*,
670   *427–428*, 191–202. https://doi.org/10.1016/j.scitotenv.2012.04.030

671 Nagar, P. K., Singh, D., Sharma, M., Kumar, A., Aneja, V. P., George, M. P., Agarwal, N., & Shukla, S. P. (2017).
672   Characterization of PM2.5 in Delhi: role and impact of secondary aerosol, burning of biomass, and municipal
673   solid waste and crustal matter. *Environmental Science and Pollution Research*, *24*(32), 25179–25189.
674   https://doi.org/10.1007/s11356-017-0171-3

675 Nault, B. A., Campuzano-Jost, P., Day, D. A., Guo, H., Jo, D. S., Handschy, A. V., Pagonis, D., Schroder, J. C.,
676   Schueneman, M. K., Cubison, M. J., Dibb, J. E., Hodzic, A., Hu, W., Palm, B. B., & Jimenez, J. L. (2020).
677   Interferences with aerosol acidity quantification due to gas-phase ammonia uptake onto acidic sulfate filter
678   samples. *Atmospheric Measurement Techniques*, *13*(11), 6193–6213. https://doi.org/10.5194/amt-13-6193-
679   2020

680 Nicolás, J. F., Galindo, N., Yubero, E., Pastor, C., Esclapez, R., & Crespo, J. (2009). Aerosol inorganic ions in a
681   semiarid region on the Southeastern Spanish mediterranean coast. *Water, Air, and Soil Pollution*, *201*(1–4),

682   149–159. https://doi.org/10.1007/s11270-008-9934-2

683   Nie, W., Wang, T., Gao, X., Pathak, R. K., Wang, X., Gao, R., Zhang, Q., Yang, L., & Wang, W. (2010).
684   Comparison among filter-based, impactor-based and continuous techniques for measuring atmospheric fine
685   sulfate and nitrate. *Atmospheric Environment*, *44*(35), 4396–4403.
686   https://doi.org/10.1016/j.atmosenv.2010.07.047

687   Pakkanen, T. A., & Hillamo, R. E. (2002). Comparison of sampling artifacts and ion balances for a Berner low-
688   pressure impactor and a virtual impactor. *Boreal Environment Research*, *7*(2), 129–140.

689   Pandolfi, M., Querol, X., Alastuey, A., Jimenez, J. L., Jorba, O., Day, D., Ortega, A., Cubison, M. J., Comerón, A.,
690   Sicard, M., Mohr, C., Prévôt, A. S. H., Minguillón, M. C., Pey, J., Baldasano, J. M., Burkhart, J. F., Seco, R.,
691   Peñuelas, J., Van Drooge, B. L., … Szidat, S. (2014). Effects of sources and meteorology on particulate matter
692   in the Western Mediterranean Basin: An overview of the DAURE campaign. *Journal of Geophysical*
693   *Research*, *119*(8), 4978–5010. https://doi.org/10.1002/2013JD021079

694   Pant, P., Shukla, A., Kohl, S. D., Chow, J. C., Watson, J. G., & Harrison, R. M. (2015). Characterization of ambient
695   PM2.5 at a pollution hotspot in New Delhi, India and inference of sources. *Atmospheric Environment*, *109*,
696   178–189. https://doi.org/10.1016/j.atmosenv.2015.02.074

697   Panteliadis, P., Helmink, H. J. P., Koopman, P. C., Hoonhout, M., Jonge, D. De, & Visser, J. H. (2012). *PM 10*
698   *sampling inlets comparison : EPA vs EU*. *12341*(1999), 12341.

699   Park, S. S., Cho, S. Y., Jo, M. R., Gong, B. J., Park, J. S., & Lee, S. J. (2014). Field evaluation of a near-real time
700   elemental monitor and identification of element sources observed at an air monitoring supersite in Korea.
701   *Atmospheric Pollution Research*, *5*(1), 119–128. https://doi.org/10.5094/APR.2014.015

702   Patel, A., Rastogi, N., Gandhi, U., & Khatri, N. (2021). Oxidative potential of atmospheric PM10 at five different
703   sites of Ahmedabad, a big city in Western India. *Environmental Pollution*, *268*, 115909.
704   https://doi.org/10.1016/j.envpol.2020.115909

705   Pathak, R. K., & Chan, C. K. (2005). Inter-particle and gas-particle interactions in sampling artifacts of PM2.5 in
706   filter-based samplers. *Atmospheric Environment*, *39*(9), 1597–1607.
707   https://doi.org/10.1016/j.atmosenv.2004.10.018

708   Peck, J., Gonzalez, L. A., Williams, L. R., Xu, W., Croteau, P. L., Timko, M. T., Jayne, J. T., Worsnop, D. R.,
709   Miake-Lye, R. C., & Smith, K. A. (2016). Development of an aerosol mass spectrometer lens system for
710   PM2.5. *Aerosol Science and Technology*, *50*(8), 781–789. https://doi.org/10.1080/02786826.2016.1190444

711   Pope, C. A., Ezzati, M., & Dockery, D. W. (2009). Fine-Particulate Air Pollution and Life Expectancy in the United
712   States. *New England Journal of Medicine*, *360*(4), 376–386. https://doi.org/10.1056/nejmsa0805646

Querol, X., Pey, J., Minguillón, M. C., Pérez, N., Alastuey, A., Viana, M., Moreno, T., Bernabé, R. M., Blanco, S., Cárdenas, B., Vega, E., Sosa, G., Escalona, S., Ruiz, H., & Artíñano, B. (2008). PM speciation and sources in Mexico during the MILAGRO-2006 campaign. *Atmospheric Chemistry and Physics*, *8*(1), 111–128. https://doi.org/10.5194/acp-8-111-2008

Rai, P., Furger, M., El Haddad, I., Kumar, V., Wang, L., Singh, A., Dixit, K., Bhattu, D., Petit, J. E., Ganguly, D., Rastogi, N., Baltensperger, U., Tripathi, S. N., Slowik, J. G., & Prévôt, A. S. H. (2020). Real-time measurement and source apportionment of elements in Delhi's atmosphere. *Science of the Total Environment*, *742*. https://doi.org/10.1016/j.scitotenv.2020.140332

Rai, P., Slowik, J. G., Furger, M., El Haddad, I., Visser, S., Tong, Y., Singh, A., Wehrle, G., Kumar, V., Tobler, A. K., Bhattu, D., Wang, L., Ganguly, D., Rastogi, N., Huang, R. J., Necki, J., Cao, J., Tripathi, S. N., Baltensperger, U., & Prevot, A. S. H. (2021). Highly time-resolved measurements of element concentrations in PM10 and PM2.5: Comparison of Delhi, Beijing, London, and Krakow. *Atmospheric Chemistry and Physics*, *21*(2), 717–730. https://doi.org/10.5194/acp-21-717-2021

Rastogi, N., & Sarin, M. M. (2005). Long-term characterization of ionic species in aerosols from urban and high-altitude sites in western India: Role of mineral dust and anthropogenic sources. *Atmospheric Environment*, *39*(30), 5541–5554. https://doi.org/10.1016/j.atmosenv.2005.06.011

Rengarajan, R., Sarin, M. M., & Sudheer, A. K. (2007). Carbonaceous and inorganic species in atmospheric aerosols during wintertime over urban and high-altitude sites in North India. *Journal of Geophysical Research Atmospheres*, *112*(21), 1–16. https://doi.org/10.1029/2006JD008150

Schaap, M., Spindler, G., Schulz, M., Acker, K., Maenhaut, W., Berner, A., Wieprecht, W., Streit, N., Müller, K., Brüggemann, E., Chi, X., Putaud, J. P., Hitzenberger, R., Puxbaum, H., Baltensperger, U., & Ten Brink, H. (2004). Artefacts in the sampling of nitrate studied in the "iNTERCOMP" campaigns of EUROTRAC-AEROSOL. *Atmospheric Environment*, *38*(38), 6487–6496. https://doi.org/10.1016/j.atmosenv.2004.08.026

Sharma, D., & Kulshrestha, U. C. (2014). Spatial and temporal patterns of air pollutants in rural and urban areas of India. *Environmental Pollution*, *195*(2), 276–281. https://doi.org/10.1016/j.envpol.2014.08.026

Sharma, S. K., Mandal, T. K., Jain, S., Saraswati, Sharma, A., & Saxena, M. (2016). Source Apportionment of PM2.5 in Delhi, India Using PMF Model. *Bulletin of Environmental Contamination and Toxicology*, *97*(2), 286–293. https://doi.org/10.1007/s00128-016-1836-1

Shukla, A. K., Lalchandani, V., Bhattu, D., Dave, J. S., Rai, P., Thamban, N. M., Mishra, S., Gaddamidi, S., Tripathi, N., Vats, P., Rastogi, N., Sahu, L., Ganguly, D., Kumar, M., Singh, V., Gargava, P., & Tripathi, S. N. (2021). Real-time quantification and source apportionment of fine particulate matter including organics and elements in Delhi during summertime. *Atmospheric Environment*, *261*(July), 118598. https://doi.org/10.1016/j.atmosenv.2021.118598

746 Singh, A., Rastogi, N., Kumar, V., Slowik, J. G., Satish, R., Lalchandani, V., Thamban, N. M., Rai, P., Bhattu, D.,
747   Vats, P., Ganguly, D., Tripathi, S. N., & Prévôt, A. S. H. (2021). Sources and characteristics of light-absorbing
748   fine particulates over Delhi through the synergy of real-time optical and chemical measurements. *Atmospheric*
749   *Environment*, *252*(March). https://doi.org/10.1016/j.atmosenv.2021.118338

750 Singh, A., Satish, R. V., & Rastogi, N. (2019). Characteristics and sources of fine organic aerosol over a big semi-
751   arid urban city of western India using HR-ToF-AMS. *Atmospheric Environment*, *208*(April), 103–112.
752   https://doi.org/10.1016/j.atmosenv.2019.04.009

753 Singhai, A., Habib, G., Raman, R. S., & Gupta, T. (2017). Chemical characterization of PM1.0 aerosol in Delhi and
754   source apportionment using positive matrix factorization. *Environmental Science and Pollution Research*,
755   *24*(1), 445–462. https://doi.org/10.1007/s11356-016-7708-8

756 Takahama, S., Wittig, A. E., Vayenas, D. V., Davidson, C. I., & Pandis, S. N. (2004). Modeling the diurnal variation
757   of nitrate during the Pittsburgh Air Quality Study. *Journal of Geophysical Research D: Atmospheres*, *109*(16).
758   https://doi.org/10.1029/2003JD004149

759 Tobler, A., Bhattu, D., Canonaco, F., Lalchandani, V., Shukla, A., Thamban, N. M., Mishra, S., Srivastava, A. K.,
760   Bisht, D. S., Tiwari, S., Singh, S., Močnik, G., Baltensperger, U., Tripathi, S. N., Slowik, J. G., & Prévôt, A.
761   S. H. (2020). Chemical characterization of PM2.5 and source apportionment of organic aerosol in New Delhi,
762   India. *Science of the Total Environment*, *745*. https://doi.org/10.1016/j.scitotenv.2020.140924

763 Tremper, A. H., Font, A., Priestman, M., Hamad, S. H., Chung, T. C., Pribadi, A., Brown, R. J. C., Goddard, S. L.,
764   Grassineau, N., Petterson, K., Kelly, F. J., & Green, D. C. (2018). Field and laboratory evaluation of a high
765   time resolution x-ray fluorescence instrument for determining the elemental composition of ambient aerosols.
766   *Atmospheric Measurement Techniques*, *11*(6), 3541–3557. https://doi.org/10.5194/amt-11-3541-2018

767 USEPA, & Etv. (2012). *Environmental Technology Verification Report Cooper Environmental Services LLC † Xact*
768   *625 Particulate Metals Monitor*. *September 2012*. http://cooperenvironmental.com/

769 Viana, M., Chi, X., Maenhaut, W., Cafmeyer, J., Querol, X., Alastuey, A., Mikuška, P., & Večeřa, Z. (2006).
770   Influence of sampling artefacts on measured PM, OC, and EC levels in carbonaceous aerosols in an urban
771   area. *Aerosol Science and Technology*, *40*(2), 107–117. https://doi.org/10.1080/02786820500484388

772 Wang, M., Aaron, C. P., Madrigano, J., Hoffman, E. A., Angelini, E., Yang, J., Laine, A., Vetterli, T. M., Kinney, P.
773   L., Sampson, P. D., Sheppard, L. E., Szpiro, A. A., Adar, S. D., Kirwa, K., Smith, B., Lederer, D. J., Diez-
774   Roux, A. V., Vedal, S., Kaufman, J. D., & Barr, R. G. (2019). Association between long-term exposure to
775   ambient air pollution and change in quantitatively assessed emphysema and lung function. *JAMA - Journal of*
776   *the American Medical Association*, *322*(6), 546–556. https://doi.org/10.1001/jama.2019.10255

777 Wu, W. S., & Wang, T. (2007). On the performance of a semi-continuous PM2.5 sulphate and nitrate instrument

778    under high loadings of particulate and sulphur dioxide. *Atmospheric Environment*, *41*(26), 5442–5451.

779    https://doi.org/10.1016/j.atmosenv.2007.02.025

780  Zhang, D., Shi, G. Y., Iwasaka, Y., & Hu, M. (2000). Mixture of sulfate and nitrate in coastal atmospheric aerosols:

781    Individual particle studies in Qingdao (36°04'N, 120°21'E), China. *Atmospheric Environment*, *34*(17), 2669–

782    2679. https://doi.org/10.1016/S1352-2310(00)00078-9

783  Zhang, X., & Mcmurryt, P. H. (1992). EVAPORATIVE LOSSES OF FINE PARTICULATE NITRATES DURING

784    SAMPLING. In *Atmospheric Environment* (Vol. 26, Issue 18).

785